# Selective placement of magnetic $Fe_3O_4$ nanoparticles into the lamellar nanostructure of PS-*b*-PMMA diblock copolymer

I. Barandiaran[1], G. Kortaberria[1*]

[1] "Materials + Technologies" Group, Universidad del Pais Vasco/Euskal Herriko Unibertsitatea, Plaza Europa 1, 20018 Donostia, Spain

*corresponding autor: Galder Kortaberria, Plaza Europa 1, 20018 Donostia, Spain. Tel: 0034 943017171; email: galder.cortaberria@ehu.es

## ABSTRACT

The aim of this work is to obtain a good and selective dispersion of $Fe_3O_4$ magnetic nanoparticles into the lamellar morphology of PS-*b*-PMMA diblock copolymer. The addition of unmodified nanoparticles inhibited the formation of the lamellar nanostructure obtained for the neat copolymer. Nanoparticles were then modified with 3-methacryloxypropyltrimethoxysilane (MPTS) in order to increase compatibility with PMMA block. Modification was probed by infrared spectroscopy and thermogravimetric analysis, while morphologies were analyzed by atomic force microscopy. Lamellar morphology was maintained but big nanoparticle agglomerates were found. Finally, nanoparticles were modified with PMMA brushes by *grafting through* technique, obtaining nanocomposites with lamellar morphology in which modified nanoparticles were selectively placed into PMMA domains of the block copolymer. For the nanocomposite with the higher nanoparticle amount, lamellar morphology started to change from lamellar to a mixture of lamellar and hexagonally packed cylinders, probably due to the change in volume fraction among blocks promoted by the presence of a higher amount of nanoparticles in PMMA domains.

## 1. INTRODUCTION

Engineering the self-assembly of inorganic nanoparticles within block copolymer nanodomains is useful for the design of periodic structures to form materials with enhanced mechanical strength as well as to achieve unique optical, electronic and magnetic properties at the nanometer scale, for applications in solar cells, catalysts or high density magnetic storage media. Block copolymers are a versatile platform material because they can self-assemble into various periodic structures for proper compositions and under adequate conditions, owing to the microphase separation between dissimilar blocks [1-3]. To overcome the problem of the tendency of nanoparticles to aggregate due to their high surface area and surface energy and to facilitate their dispersion in a selected block of a block copolymer different routes have been used [1, 3-5]. One of them has

been the use of surfactants. In that way, Peponi et al [1] used surfactants to disperse conductive silver nanoparticles in the desired domains of poly(styrene-*b*-butadiene-*b*-styrene) (SBS) copolymer. Emrick et al [4] controlled the surface hydrophobicity by using different surfactants in order to disperse CdSe nanoparticles in poly(styrene-*b*-2-vinylpiridine) (PS-*b*-P2VP) copolymer, creating hierarchically ordered patterns with CdSe nanoparticles located in PS or P2VP domains depending on the surfactant. Electrophoretic deposition of nanoparticles [5] has been another method to disperse nanoparticles. Zhang et al [5] used this method for placing CdSe nanoparticles in diblock copolymer templates. The so-called *in situ* approach has also been used by several authors [6-9] for incorporating inorganic nanoparticles into block copolymer nanostructures: nanoparticles are directly synthesized within a block copolymer domain from metal precursors. Preformed micelles of block copolymers containing metal precursors are used as nanoreactors to synthetize nanoparticles selectively in block copolymers. Due to its chemical affinity, the salt selectively infiltrates the hydrophilic copolymer domain. Nanoparticles then form selectively, upon reduction within the precursor-loaded domains. In that way Chan et al [6] prepared nanocomposites with block copolymers and Pb or Pt nanoparticles. Saito et al [7, 8] synthesized silver nanoparticles in the lamellar and spherical domains of PS-*b*-P2VP copolymer. Cohen et al [9] prepared nanocomposites based on poly(styrene-b-acrylic acid) (PS-*b*-PAA) copolymer and metallic nanoparticles of Pd, Cu, Au and Ag.

Among different methods used for dispersing nanoparticles into block copolymers, one of the most effective ones is the grafting of polymers either through physical adsorption [10, 11] or by covalent bonding of the polymer chain [12-14]. Non-covalent physisorption makes the processing of particles difficult and hence, covalent bonding is preferable in many cases [12]. There are essentially three techniques to chemically graft polymers on nanoparticles surface: *grafting to* [15-17], *grafting from* [18-20] and *grafting through* [21-27]. In the *grafting through* technique, molecules attached to the surface also present a group suitable for polymerization (usually a silane with terminal vinyl groups, which are subsequently used for the polymerization). Nanoparticles present in the polymerization medium are covered by the polymer. Obtained grafting densities are usually higher than those obtained by *grafting to* and the technique is easier to carry out than *grafting from* one. As nanoparticle surface is multifunctional, polymeric chains also present bonds among them, creating a sort of network [28].

On the other hand, magnetic nanoparticles have received special attention due to its potential applications in many diverse fields such as ferrofluids, magnetic resonance imagining, biomedicine and drug delivery [29-32]. Magnetic nanoparticles assembly into block copolymers has gained attention as a method to fabricate hybrid materials with magnetic properties [17, 33-36]. In this way, Park et al [33,34] assembled $Fe_2O_3$ nanoparticles in poly(styrene-b-isoprene) (PS-*b*-PI) copolymer, finding a change in the morphology obtained from hexagonal cylinders to body-centered cubic. Lauter-Pasyuk et al [35] prepared nanocomposites with $Fe_3O_4$ and poly(styrene-*b*-butylmethacrylate) (PS-*b*-PBMA) copolymer, obtained a mixed morphology of perpendicular and parallel lamellae on the surface, with unknown nanoparticle location. Barandiaran et al [17] prepared nanocomposites based on poly(styrene-*b*-caprolactone) (PS-*b*-PCL) and $Fe_3O_4$ nanoparticles modified with PMMA-*b*-PCL brushes by *grafting to* technique, obtaining good dispersion of nanoparticles, which were placed at the interfaces. Xu et al [36] prepared nanocomposites with poly(styrene-*b*-methylmethacrylate) (PS-*b*-PMMA) copolymer and $Fe_3O_4$ nanoparticles modified with PMMA brushes of different molecular weights by *grafting from* technique, analyzing the effect of brush length and nanoparticle content on the morphology and dispersion level of nanoparticles.

In this work, $Fe_3O_4$ nanoparticles have been modified with PMMA brushes by *grafting through* technique, for being dispersed into annealed PS-*b*-PMMA copolymer thin films. In contrast with nanocomposites prepared with pristine nanoparticles or those modified with silane, no significant agglomerates were found, and nanoparticles were selectively placed at PMMA lamellae, without disrupting copolymer morphology.

## 2. EXPERIMENTAL

### 2.1. Materials

Magnetite ($Fe_3O_4$) nanoparticles with a nominal size of 9 nm were purchased from Integram Technologies, Inc.. 3-methacryloxypropyltrimethoxysilane, with 98% of purity, was purchased from ABCR. The initiator 2,2'-azobisisobutyronitrile (AIBN), used without further purification, and methylmethacrylate (MMA) monomer, with a purity of 99 %, distilled under reduced pressure over $CaH_2$ before use, was purchased from Aldrich. Poly(styrene-*b*-methyl methacrylate) (PS-*b*-PMMA) block copolymer ($f_{PS}=f_{PMMA}= 0.5$) was purchased from Polymer Source, Inc.. The number average

molecular weight of both PS and PMMA blocks is 80.000 g/mol, with a polydispersity of 1.09.

## 2.2. Nanoparticle modification

### 2.2.1. Silanization process

$Fe_3O_4$ nanoparticles were first modified with MPTS. Scheme 1 shows the reaction scheme of the silanization process. This reaction implies a nucleophilic attack of –OH groups at nanoparticle surface to the Si atoms of MPTS. 0.05 g of nanopaticles and 10 μmol of silane were mixed by sonication into 40 mL of toluene. The reaction was carried out at inert atmosphere for 3 hours at 60 ºC. Nanoparticles were subsequently washed with THF and dried in vacuum for 72 h at 40 ºC.

### 2.2.2. Grafting through process

Once the magnetite nanoparticles were silanized, the modification of nanoparticles surface with PMMA brushes by *grafting through* method was carried out, as it can be seen in Scheme 1. 0.02 g of silanized $Fe_3O_4$ nanoparticles and 0.1 g of AIBN were dispersed into 40 mL of toluene and then 2 mL of monomer were added. The reaction was carried out at inert $N_2$ atmosphere at 70 ºC for 5 h. Modified nanoparticles were subsequently washed with THF and dried in vacuum for 72 h at 40 ºC.

## 2.3. Nanocomposite preparation

Nanocomposites were prepared mixing PS-*b*-PMMA block copolymer with unmodified, silanized and polymer-modified $Fe_3O_4$ nanoparticles. Nanoparticles were first dispersed in toluene for two hours by sonication, followed by PS-*b*-PMMA block copolymer addition. Thin films were then prepared by spin-coating onto Si(100) wafers at 2000 rpm for 30 s using a Telstar Instrumat P-6708D spin-coater. The film thickness as measured by AFM after sample scratching was around 100 nm for all investigated samples. For selective solvent annealing, thin films were exposed to saturated acetone vapors (selective for PMMA, with $\chi_{PMMA} = 0.18$ and $\chi_{PS} = 1.1$ [37]) for 16 h in a closed vessel and kept at room temperature following spin-coating, without removing the residual solvent. After exposure samples were removed and stored at room atmosphere before characterization. This exposure time was chosen in order to obtain a lamellar morphology for the neat copolymer. Nanocomposites were prepared with 1, 2, and 5 wt% of nanoparticles.

## 2.4. Characterization techniques

Fourier transformed infrared spectroscopy (FTIR) was carried out with a Nicolet Nexus 600 FTIR spectrometer, performing 20 scans with a resolution of 4 cm$^{-1}$.

Thermogravimetric analysis (TGA) was performed with a Mettler Toledo TGA/SDTA851 instrument. Tests were carried out from room temperature to 750 ºC with a heating rate of 10 ºC/min.

Surface morphologies obtained for different films were studied by atomic force microscopy with a scanning probe microscopy AFM Dimension ICON of Bruker, operating in tapping mode (TM–AFM). An integrated silicon tip/cantilever, from the same manufacturer, having a resonance frequency of around 300 kHz, was used. Measurements were performed at a scan rate of 1 Hz/s, with 512 scan lines.

## 3. RESULTS AND DISCUSSION

### 3.1. Nanocomposites with silanized nanoparticles

Magnetic nanoparticles were first surface-modified with MPTS silane in order to increase their compatibility with PS-*b*-PMMA copolymer, and also for grafting the initiator for the polymerization of PMMA brushes, following a procedure shown in the first part of Scheme 1. The success of silanization process was probed by FTIR and TGA measurements, as it can be seen in Figure 1. From FTIR spectra, the appearance of bands related with the main bonds of MPTS compound can be seen (C-O-C, Si-O-C, C=C, or C=O) indicated in the inner part of Figure 1A. The presence of those bands, absent in the spectrum of unmodified nanoparticles, indicate the presence of MPTS attached to the surface. TGA measurements, besides showing the modification of the nanoparticles with the organic compound, were used to determine the amount of grafted silane [38]. The surface density of the silane was about 2.8 molecules/nm$^2$. A direct comparison of the surface density of hydroxyl groups (8.1 molecules/nm$^2$) and that of the silane on the surface yielded a reaction efficiency of 34.5 %. Surface morphologies of obtained nanocomposite films have been analyzed in terms of AFM. Figure 2 shows AFM images of neat PS-*b*-PMMA copolymer and nanocomposites with 1 and 2 wt% of silane-modified nanoparticles. The brighter regions in the phase contrast AFM image correspond to the PMMA block because PMMA has a higher modulus than PS chain at room temperature [37, 39]. For neat copolymer, surface perpendicular lamellar microphase morphology can

be seen, with an average interlamellar distance of 77 nm. PMMA and PS lamellae are 68 and 8 nm width, respectively. This morphology is the typical equilibrium state phase structure in thin symmetric diblock copolymer films [37]. As was pointed out by several authors [37, 40] ordered microphase morphology can be obtained by exposing films to selective solvent vapor good for PMMA. Previous works [37, 40-44] have shown that when PS-*b*-PMMA is cast on a silicon wafer, PMMA segregates to the surface while PS segregates to the air interface. So after spin-coating seems that PMMA dominates in the substrate interface while PS is placed mainly at the free surface. Since PMMA is more soluble in acetone than PS, there is a strong attraction between polymer and solvent, while the net interaction between polymer segments is repulsive. So polymer chains start to swell when they are in contact with solvent. Diffusion of solvent to the surface plays an important role in obtained morphology. In this way, for PS-*b*-PMMA, Xuan et al [37] proposed a mechanism of solvent vapor annealing for PMMA selective solvents. Taking all this into account, several microphase-separated morphologies have been observed by different authors for PS-*b*-PMMA depending on exposure time and film thickness: hexagonally packed nanocylinders, striped or lamellar morphologies.

In our case, as the aim was to obtain the typical equilibrium lamellar morphology, an exposure time of 16 h was performed in acetone vapors, achieving the desired morphology, as shown in Figure 2. Regarding the effect of silane-modified nanoparticles, as it can be seen in the AFM images, the lamellar morphology was maintained with nanoparticle addition. Big nanoparticle agglomerates appeared, however. Those agglomerates tended to PMMA domains but their size was bigger than that of PMMA lamellae. As a good and selective dispersion of magnetic nanofillers was not obtained, the following step was their modification with PMMA brushes for increasing the compatibility with one of the blocks.

## 3.2. Nanocomposites with nanoparticles with PMMA brushes

After silanization, nanoparticles were modified with PMMA brushes by *grafting through* method, as was shown in Scheme 1. The presence of brushes in the surface was probed by FTIR and TGA. Main bands related to PMMA bonds (C=O, C-O-C, etc) can be seen in the FTIR spectrum of Figure 3A. TGA thermogram of nanoparticles modified with brushes can be seen in Figure 3B, compared with that of pristine and silanized ones. The weight loss related to the degradation of PMMA can be clearly seen, thus probing the presence of the polymer in the sample. As the cleavage of PMMA brushes from the

nanoparticles has not been possible [26], in order to obtain an approximation of the molecular weight of PMMA chains, as in a previous work [26], a polymerization at the same conditions but without the presence of nanoparticles in the media was carried out. Molecular weight obtained for PMMA chains after 5 h reaction was around 15,000, so we can also expect that the PMMA brushes have the same molecular weight. In these nanoparticles the molecular weight of the PMMA chains is lower than that of the PMMA block chains. Being the chains smaller, a better wetting by PMMA block chains could be expected [45]. Surface morphology of nanocomposite films was analyzed by AFM. Figure 4 shows AFM images of nanocomposites with 2 and 5 wt% of nanoparticles. Lamellar morphology is maintained for nanocomposites with 1 (not shown here) and 2 wt%, though lamellae are not so regular and parallel among them as were for the neat copolymer. In the same way, the width of PMMA lamellae increased probably due to the nanoparticles placed on them. There are no remarkable agglomerates in the nanocomposites, indicating that dispersion has been improved with PMMA brushes. In the height image the presence of nanoparticles at PMMA domains can be noticed. Moreover, as indicative of the presence of nanoparticles, for the nanocomposite with 5 wt% of nanoparticles, the morphology started to change and a mixture of lamellae and perpendicular hexagonally packed cylinders (circles in Figure 4B1) can be seen. This fact indicates that nanoparticles, located at PMMA domains, alter the volume fraction among blocks, altering the equilibrium morphology. As more nanoparticles are located at PMMA domains, the volume of those has increased, altering the volume ratio among blocks and promoting the morphology change. This change in morphology promoted by the specific location nanoparticles in one block has been found by other authors [36, 40]. As an example, Gutierrez et al [40] found that PS-*b*-PMMA copolymer thin films, annealed with acetone vapors for 48 h, change their morphology from hexagonal packed cylinders to lamellar and striped structure with 5 and 10 w% of $TiO_2$ nanoparticles, respectively. Xu et al [36] dispersed magnetic nanoparticles with PMMA brushes of different molecular weight in PS-*b*-PMMA films thermally annealed. For around 4 wt% of nanoparticles with the lowest molecular weight brushes (2700), the morphology changed from perpendicular lamellae to a mixture of perpendicular and parallel ones, frustrating the assembly of lamellar structure for contents higher than 10 wt%. Upon increasing molecular weight of brushes (35700), nanoparticles tended to aggregate, the copolymer assembling into onionlike rings around them. In our case, nanoparticles with PMMA brushes of 15,000 have been used, varying their amount from 1 to 5 wt%. With this

molecular weight and nanoparticle amount, morphology started to change between 2 and 5 wt% with no remarkable agglomerates that could frustrate the assembly.

In order to clearly show the improvement of dispersion and selective placement of nanoparticles by modifying them with PMMA brushes, Figure 5 shows AFM images of nanocomposites prepared with 2 wt% of pristine nanoparticles, silanized ones and those with PMMA brushes. Pristine nanoparticles frustrate the assembly of the copolymer, as it can be seen in Figure 5A. Once they were functionalized with MPTS, the lamellar morphology of the copolymer was achieved but nanoparticles tended to aggregate, as it can be seen in Figure 5B. Finally, when they were surface modified with PMMA brushes, nanoparticles were well dispersed and selectively placed at PMMA domains maintaining lamellar morphology for 1 and 2 wt% nanocomposites. As mentioned above, for nanocomposites with 5 wt% of nanoparticles, the morphology started to change to cylinders, presenting a mixture of lamellar and cylindrical morphology.

In the 3D AFM images of the thin film nanocomposites shown in Figure 6 the effect of nanoparticles on the morphology of the block copolymer can be seen more clearly. As it can be seen in Figure 6A, corresponding to the neat block copolymer, the height of the lamellae is continuous, with no appreciable discontinuity in them. When silane-modified nanoparticles are added (Figure 6B) the appearance of hills can be seen, located in the PMMA domains. Apart from these hills the height of the PMMA lamellas can be considered as continuous. These hills could represent small aggregates of $Fe_3O_4$ nanoparticles modified with MPTS silane, present at PMMA domains due to their improved affinity. However, a good dispersion was not achieved, as their presence through the rest of the PMMA domains was negligible. Figures 6C and 6D show 3D AFM images for nanocomposites with 2 and 5 wt% of nanoparticles with brushes. The presence of the nanoparticles can be seen, as small points standing out from the PMMA domains. The height of lamellae was not more continuous, with nanoparticles well located through all PMMA domains, confirming the improvement of dispersion. Comparing the images of nanocomposites with 2 and 5 wt%, previously shown morphology change was confirmed. With the lowest concentration lamellar morphology was maintained, while when the concentration increased the morphology was between lamellar and cylindrical, as it was previously pointed out. In Figure 7 the profile images of neat block copolymer (Fig. 7A), nanocomposites with 2 wt% of silanized nanoparticles (Fig. 7B) and PMMA modified nanoparticles (Fig. 7C) can be seen. In these profile images the effect of the

nanoparticles in the PMMA domain of the copolymer can be clearly seen, how the neat copolymer PMMA domains are continuous, how the silanized nanoparticle addition creates some hills on the lamellae and the addition of PMMA modified nanoparticles are well dispersed on PMMA domains.

Figure 8 shows the AFM image of the charred nanocomposite film containing 5 wt% nanoparticles as an example, in order to better visualize them and have an approximate idea of their average size. Nanoparticle size varied from around 20 to 45 nm for all the nanocomposites studied, smaller than the size of PMMA domains in which they are located. It is clear that some nanoparticles appear together since their nominal diameter is 9 nm. These measurements agree with the ones obtained from the profile images of Figure 7B. Those small aggregates probably were formed during functionalization and not during nanocomposite preparation or during annealing. In the *grafting through* functionalization method, the polymerization was carried out with silane-modified nanoparticles in the media and, distinctly from the *grafting from* method, where the polymer chain grows only from the surface of the nanoparticle, the functional group located in the surface of the nanoparticle could join a growing PMMA chain in which there could be more nanoparticles previously joined. As the surface of the nanoparticles is multifunctional, with several double bonds, several chains could be bonded to different nanoparticles [27, 46]. Due to these reasons it is supposed that nanoparticles, instead of being located individually, are bonded together with several polymer chains, creating a kind of network formed by nanoparticles and PMMA chains.

## 4. CONCLUSIONS

The following conclusions can be extracted from the synthesis and characterization of nanocomposite thin films based on PS-*b*-PMMA copolymer and $Fe_3O_4$ nanoparticles. The copolymer films were annealed by exposure to acetone (selective for PMMA) vapors for 16 h in order to obtain classical lamellar morphology. For nanocomposites with pristine nanoparticles lamellar morphology was disrupted due to the low compatibility among matrix and fillers. Nanoparticles were then successfully surface-modified with MPTS silane in order to increase their compatibility with PMMA domains. Lamellar morphology of films was maintained with nanoparticle adding but they tended to agglomerate. In order to better disperse and selectively place nanoparticles, they were modified with PMMA brushes by *grafting through* technique. Once modified, they were

well dispersed into PMMA domains of the copolymer films maintaining the lamellar morphology for nanocomposites with 1 and 2 wt% of nanoparticles. For higher nanoparticle amount of 5 wt% morphology started to change to a mixture of lamellas and hexagonally packed cylinders. This fact seemed to confirm the presence of nanoparticles at PMMA domains, increasing their volume and altering the volume fraction of the copolymer and consequently, the equilibrium morphology. As the size of nanoparticles in PMMA domains has been found to be bigger than that of single nanoparticles, it seems that more than one single nanoparticle was present at PMMA domains. This slight agglomeration could occur during grafting through process, in which, as was previously pointed by our group, nanoparticles, instead of being located individually, could be bonded together with several polymer chains, creating a kind of network. In any case, these agglomerates were smaller than PMMA domains, not big enough to disrupt copolymer morphology.

## ACKNOWLEDGEMENT

## REFERENCES

1. Peponi, L., Tercjak, A., Gutierrez, J., Stadler, H., Torre, L., Kenny, J. M., Mondragon, I. Self assembly of SBS copolymers as templates for conductive silver nanocomposites. *Macromol Mat Eng* 2008, 293, 568-573. DOI: 10.1002/mame.200800033

2. Lo, C. T., Lee, B., Winans, R. E., Thiyagarajan, P. Effect of dispersion of inorganic nanoparticles on the phase behavior of block copolymers in selective solvent. *Macromolecules* 2006, 39, 6318-6320. DOI: 10.1021/ma060879o

3. Lin, Y., Boker, A., He, J., Sill, K., Xiang, H., Abetz, C., Li, X., Wang, J., Balazs, A., Russel, T. P. Self-directed self-assembly of nanoparticle/block copolymer mixtures. *Nature* 2005, 434, 55-59. DOI: 10.1038/nature03310

4. Zou, S., Hong, R., Emrick, T., Walker, G. C. Ordered CdSe nanoparticles within self-assembled block copolymer domains on surfaces. *Langmuir* 2007, 23, 1612-1614. DOI: 10.1021/la0629274

5. Zhang, Q., Xu, T., Butterfield, D., Misner, M. J., Ryu, D. Y., Emrick, T., Russel, T. P. Controlled placement of CdSe nanoparticles in diblock copolymer templates by electrophoretic deposition. *Nano Lett* 2005, 5, 357-361. DOI: 10.1021/nl048103t

6. Chan, Y. C., Craig, C. S., Schrock, R. R., Cohen, R. E. Synthesis of platinum and palladium nanoclusters within microphase separated block copolymers. *Chem Mater* 1992, 4, 885-894. DOI: 10.1021/cm00022a026

7. Saito, R., Okamura, S., Ishizu, K. Introduction of colloidal silver into poly(2-vinyl pyridine) microdomain of microphase-separated poly(styrene-b-2-vynilpiridine) film. *Polymer* 1992, 33, 1099-1101. DOI: 10.1016/0032-3861(92)90029-V

8. Saito, R., Ishizu, K. Introduction of colloidal silver into poly(2-vinyl pyridine) microdomain of microphase-separated poly(styrene-b-2-vynilpiridine) film: 4. One step mehod. *Polymer* 1995, 36, 4119-4124. DOI: 10.1016/0032-3861(95)90993-C

9. Boontongkong, Y., Cohen, R. E.. Cavitated block copolymer thin films. Lateral arrays on open nanoreactors. *Macromolecules* 2002, 35, 3647-3652. DOI: 10.1021/ma0117357

10. Hadziioannou, G., Patel, S., Granik, S., Tirrel, M. Forces between surfaces of block copolymers absorbed in mica. *J Am Chem Soc* 1986, 108, 2869-2876. DOI: 10.1021/ja00271a014

11. Saleh, N., Phenrat, T., Sirk, K., Dufour, B., Ok, J., Sarbu, T., Matyjaszewski, K., Tilton, R. D., Lowry, G. V. Adsorbed triblock copolymer deliver reactive iron nanoparticles to the oil/water interface. *Nano Lett* 2005, 5, 2489-2494. DOI: 10.1021/nl0518268

12. Ladmiral, V., Morinaga, T., Ohno, K., Fukuda, T., Tsujii, Y. Synthesis of monodisperse zinc sulfide nanoparticles grafted with concentrated polystyrene brush by surface-initiated, nitroxide-mediated polymerization. *Eur Polym J* 2009, 45, 2788-2796. DOI: 10.1016/j.eurpolymj.2009.07.004

13. Synytska, A., Ionov, L., Minko, S., Motornov, M., Elchorn, K., Stamm, M., Grundle, K. Tuning wettability by controlled roughness and surface modification using core-shell particles. *Polym Mater Sci Eng* 2004, 90, 624-625

14. Wang, T. L., Yang, C. H., Shieh, Y. T., Yeh, A. C. Synthesis of CdSe-poly(n-vinyl carbazole) by atom transfer radical polymerization for potential

optoelectronic application. *Macromol Rapid Commun* 2009, 30, 1679-1683. DOI: 10.1002/marc.200900349

15. Mountrichas, G., Pispas, S., Tagmatarchis, N. Grafting to approach for functionalization of carbon nanotubes with polystyrene. *Mater Sci Eng B* 2008, 152, 40-43. DOI: 10.1016/j.mseb.2008.06.006

16. Liu, Y., Yao, Z., Adronov, A. Functionalization of single walled carbon nanotubes with well defined polymers by radical coupling. *Macromolecules* 2005, 38, 1172-1179. DOI: 10.1021/ma048273s

17. Barandiaran, I., Cappelletti, A., Strumia, M., Eceiza, A., Kortaberria, G. Generation of nanocomposites based on (PCL-b-PMMA)-grafted Fe2O3 nanoparticles and PS-b-PCL block copolymer. *Eur Polym J* 2014, 58, 226-232. DOI: 10.1016/j.eurpolymj.2014.06.022

18. Park, S. J., Cho, M. S., Lim, S. T., Choi, H. J., Jhon, M. S. Synthesis and dispersion characteristics of multi-walled carbon nanotubes composites with poly(methylmethacrylate) prepared by in situ bulk polymerization. *Macromol Rapid Commun* 2003, 24, 1070-1073. DOI: 10.1002/marc.200300089

19. Xu, G., Wu, W. T., Wang, Y., Pang, W., Zhu, Q., Wang, P., You, Y. Constructing polymer brushes on multi-walled carbon nanotubes by in situ reversible addition fragmentation chain transfer polymerization. *Polymer* 2006, 47, 5909-5918. DOI: 10.1016/j.polymer.2006.06.027

20. Xu, G., Wang, Y., Pang, W., Wu, W. T., Zhu, Q., Wang, P. Fabrication of multi-walled carbon nanotubes with polymer shells by surface RAFT polymerization. *Polym Int* 2007, 56, 847-852. DOI: 10.1002/pi.2212

21. Yang, Y., Xie, X., Wu, J., Mai, Y. W. Synthesis and self-assembly of polystyrene-grafted multiwalled carbon nanotubes with a hairy-rod nanostructure. *J Polym Sci: Part A: Polym Chem* 2006, 44, 3869-3881. DOI: 10.1002/pola.21491

22. Kim, M., Hong, C. K., Choe, S., Shim, S. E. Synthesis of polystyrene brush on multiwalled carbon nanotube treated with $KMnO_4$ in the presence of phase-transfer catalyst. *J Polym Sci Part A*: Polym Chem 2007, 45, 4413-4420. DOI: 10.1002/pola.22190

23. Du, F., Wu, K., Yang, Y., Liu, L., Gan, T., Xie, X. Synthesis and electromechanical probing of water-soluble poly(sodium-4-styrenesulfonate-co-acrylic acid)-grafted carbon nanotubes. *Nanotechnology* 2008, 19, 85716. DOI: 10.1088/0957-4484/19/8/085716

24. Roghani-Mamaqani, H., Haddadi-Asl, V., Najafi, M., Salami-Kalajahi, M. Preparation of taylor-made polystyrene composite with mixed clay anchored and free chains via atom transfer radical polymerization. *AIChe J* 2011, 57, 1873-1881. DOI: 10.1002/aic.12395

25. Etxeberria, H., Zalakain, I., Mondragon, I., Eceiza, A., Kortaberria, G. Generation of nanocomposites based on polystyrene-grafted CdSe nanoparticles by grafting through and block copolymer. *Colloid Polym Sci* 2013, 291, 1881-1886. DOI: 10.1007/s00396-013-2927-8

26. Etxeberria, H., Zalakain, I., Tercjak, A., Eceiza, A., Kortaberria, G., Mondragon, I. Functionalization of CdSe semiconductor nanoparticles with polystyrene brushes by radical polymerization. *J Nanosci Nanotechnol* 2013, 13, 643-648. DOI: 10.1166/jnn.2013.6858

27. Henze, M., Madge, D., Prucker, O., Ruhe, J. "Grafting thorugh": mechanistic aspects of radical polymerization reactions with surface-attached polymers *Macromolecules* 2014, 47, 2929-2937. DOI: 10.1021/ma402607d

28. Rahimi-Razin, S., Haddadi-Asl, V., Salami-Kalajahi, M., Behboodi-Sadabad, F., Roghani-Mamaqani, H. Matrix-grafted multiwalled carbon nanotubes/poly(methylmethacrylate) composites synthetized by in situ RAFT polymerization: a kinetic study. *Int J Chem Kinet* 2012, 44, 555-569. DOI: 10.1002/kin.20626

29. García, I., Zafeiropoulos, N.E., Janke, A., Tercjak, A., Eceiza, A., Stamm, M., Mondragon, I. Functionalization of Iron Oxide Magnetic Nanoparticles with Poly(methyl methacrylate) Brushes Via Grafting-From Atom Transfer Radical Polymerization. *Journal of Polymer Science: Part A: Polymer Chemistry* 2007, 45, 925-932. DOI: 10.1002/pola.21854

30. Kondo, A., Fukuda, H. Preparation of thermo-sensitive magnetic microspheres and their application to bioprocesses. *Colloids Surf A* 1999, 155, 435-438. DOI: S0927-7757(98)00465-8

31. Hsiao, J., Taic, M., Leed, Y., Yanga, C., Wangd, H., Liua, H., Fange, J., Chenf, S.J. Labelling of cultured macrophages with novel magnetic nanoparticles. *Magn Magn Mater* 2006, 304, e4-e6. DOI: 10.1016/j.jmmm.2006.01.134

32. Shen, H., Long, D., Zhu, L., Li, X., Dong, Y., Jia, N., Zhou, H., Xin, X., Sun, Y. Magnetic force microscopy analysis of apoptosis of HL-60 cells induced by

complex of antisense oligonucleotides and magnetic nanoparticles. *Biophys Chem* 2006, 122, 1-4. DOI: 10.1016/j.bpc.2006.01.003

33. Park, M. J., Char, K. Effect of the casting solvent on the morphology of PS-b-PI/magnetic nanoparticle mixtures. *Langmuir* 2006, 22, 1375-1378. DOI: 10.1021/la052218a

34. Park, M. J., Park, J., Hyeon, T., Char, K. Effect of interacting nanoparticles on the ordered morphology of copolymer/magnetic nanoparticle mixtures. *J Polym Sci, Part B: Polym Phys* 2006, 44, 3571—3579. DOI: 10.1002/polb.21011

35. Lauter-Pasyuk, V., Lauter, H. J., Gordeev, G. P., Muller-Buschbaum, P., Toperberg, B. P., Jernenkov, M., Petrenko, V., Aksenov, A. Parallel and perpendicular lamellar phases in copolymer/nanoparticle multilayer structures. *Physica B* 2004, 350, 939-942. DOI: 10.1016/j.physb.2004.03.265

36. Xu, C., Ohno, K., Ladmiral, V., Milkie, D. E., Kikkawa, J. M., Composto, R. J. Simultaenous block copolymer and magnetic nanoparticle assembly in nanocomposite films. *Macromolecules* 2009, 42, 1219-1228. DOI: 10.1021/ma8022266

37. Xuan, Y., Peng, J., Cui, L., Wang, H., Li, B., Han, Y. Morphology development of ultrathin symmetric diblock copolymer film via solvent vapor treatment. *Macromolecules* 2004, 37, 7301-7307. DOI: 10.1021/ma0497761

38. Bartholome, C., Beyou, E., Bourgeat-Lami, E., Chaumont, P., Zydowicz, N. Nitroxide-Mediated Polymerizations from Silica Nanoparticle Surfaces: "Graft from" Polymerization of Styrene Using a Triethoxysilyl-Terminated Alkoxyamine Initiator. *Macromolecules* 2003, 36, 7946-7952. DOI: 10.1021/ma034491u.

39. Peng, J., Wei, Y., Wang, H., Li, Y., Han, Y. Solvent induced sphere development in symmetric diblock copolymer thin films. *Macromol Rapid Commun* 2005, 26, 738-742. DOI: 10.1002/marc.200400665

40. Gutierrez, J., Garcia, I., Tercjak, A., Mondragon, I. The effect of termal and vapor annealing treatments on the self-assembly of TiO2/PS-b-PMMA nanocomposites generated via the sol-gel process. Nanotechnology 2009, 20, 225603 (9 pp). DOI: 10.1088/0957-4484/20/22/225603

41. Green, P. F., Christenson, T. M., Russell, T. P., Jerome, R. Equilibrium surface composition of diblock copolymers. *J Chem Phys* 1990, 92, 1478-1482. DOI: 10.1063/1.458106

42. Green, P. F., Christenson, T. M., Russell, T. P. Ordering at diblock copolymer surfaces. *Macromolecules* 1991, 24, 252-255. DOI: 10.1021/ma00001a038

43. Anastasiadis, S. H., Russell, T. P., Satija, S. K., Makjarzak, C. F. Neutron reflectivity studies of the surface-induced ordering of diblock copolymer films. *Phys Rev Lett* 1989, 62, 1852-1855. DOI: 0.1103/PhysRevLett.62.1852

44. Russell, T. P., Coulon, G., Deline, V. R., Miller, D. C. Characteristics of the surface-induced orientation for symmetric PS-b-PMMA diblock copolymer. *Macromolecules* 1989, 22, 4600-4606. DOI: 10.1021/ma00202a036

45. Xu, C., Ohno, K., Ladmiral, V., Composto, R. J. Dispersion of polymer-grafted magnetic nanoparticles in homopolymers and block copolymers. *Polymer* 2008, 49, 3568–3577. DOI: 10.1016/j.polymer.2008.05.040

46. Rahimi-Razin, S., Haddadi-Asl, V., Salami-Kalajahi, M., Gehgoodi-Sadabad, F., Roghani-Mamaqani, H. Matrix-grafted multiwalled carbon nanotubes/ poly(methyl methacrylate) nanocomposites synthesized by in situ RAFT polymerization: A kinetic study. *Int J Chem Kinet* 2012, 44, 555-569

**FIGURE AND SCHEME CAPTIONS**
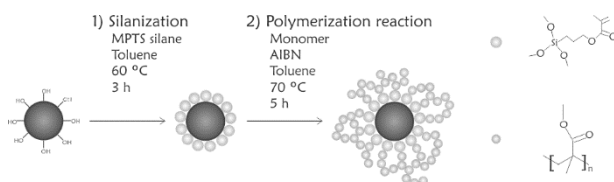


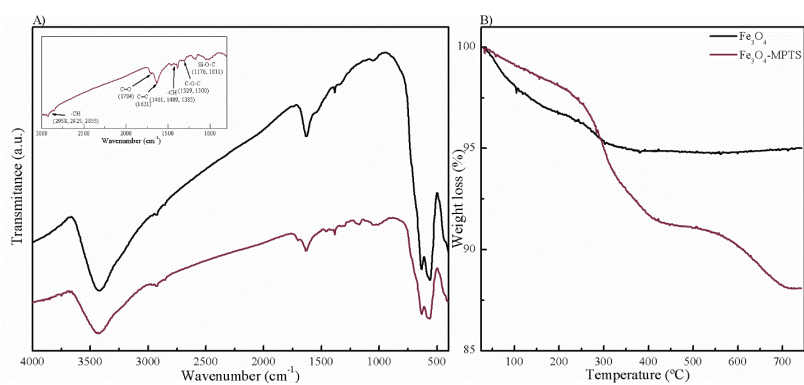**Scheme 1.** Procedure used for the silanization and grafting of PMMA brushes onto $Fe_3O_4$ nanoparticles

**Figure 1:** a) FTIR spectra of neat and silanized $Fe_3O_4$ nanoparticles. Inner spectrum shows a magnification of modified nanoparticle spectrum, and b) TGA thermogram of neat and silanized $Fe_3O_4$ nanoparticles.
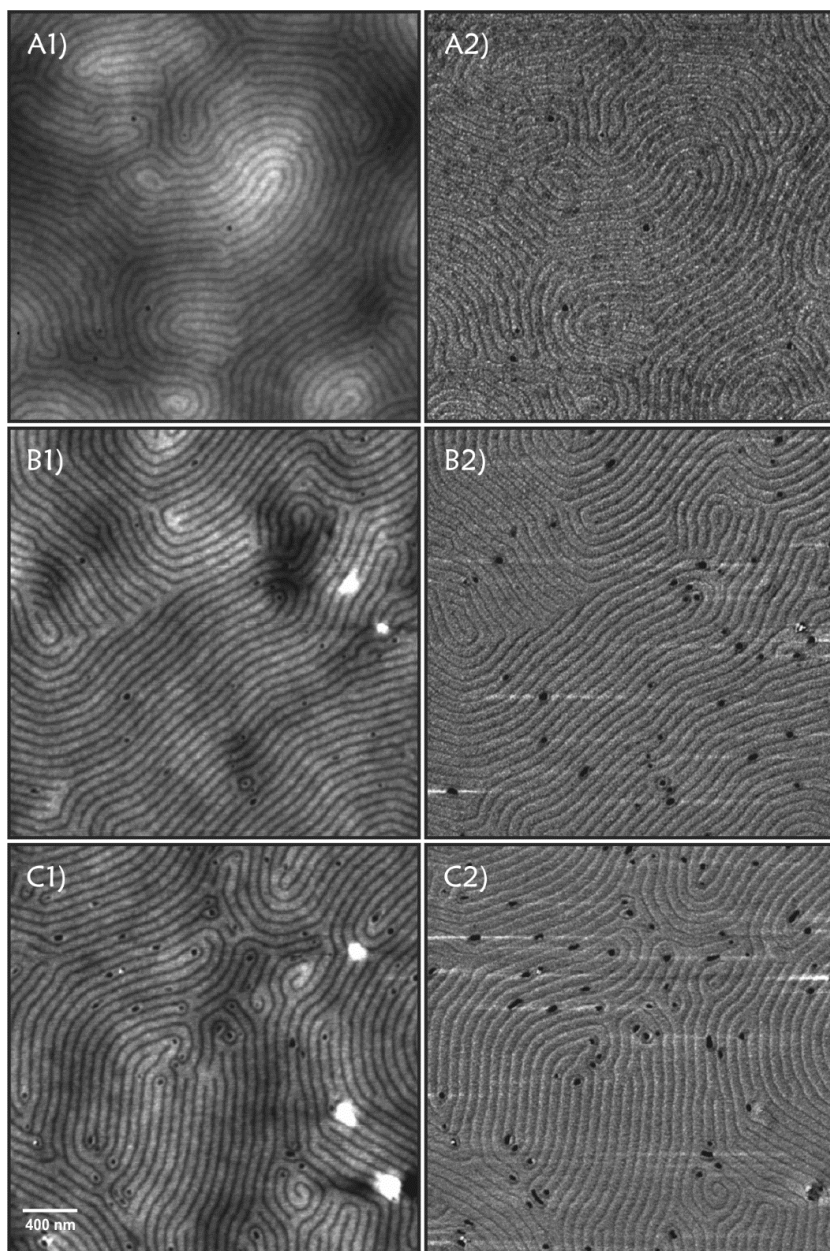
**Figure 2:** AFM (*left*/*right* height/phase) images corresponding to thin films of: a) neat PS-*b*-PMMA copolymer, b) nanocomposite with 1 wt% of silanized nanoparticles, and c) nanocomposite with 2 wt% of silanized nanoparticles, after annealing with acetone vapors for 16 h.
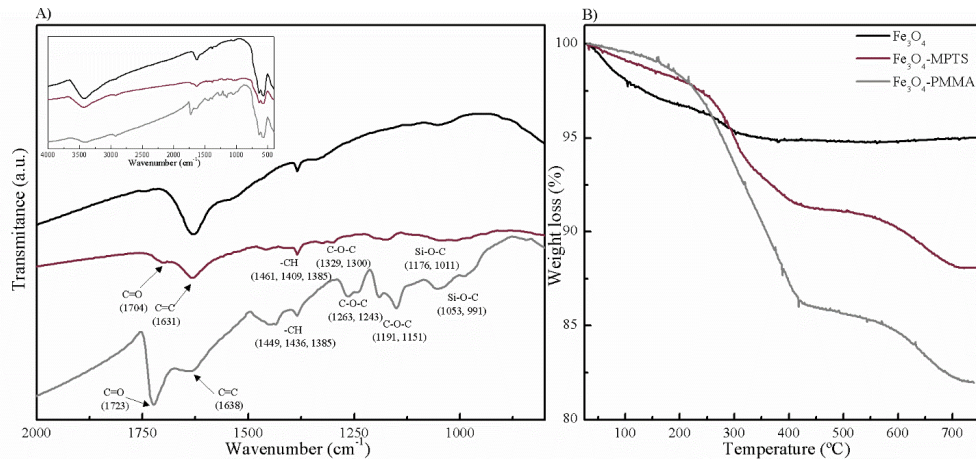
**Figure 3:** a) FTIR spectra of neat, silanized and PMMA-grafted $Fe_3O_4$ nanoparticles. Main bands are indicated by arrows. Inner spectrum shows a magnification of spectra, and b) TGA thermogram of neat, silanized and PMMA-grafted $Fe_3O_4$ nanoparticles.
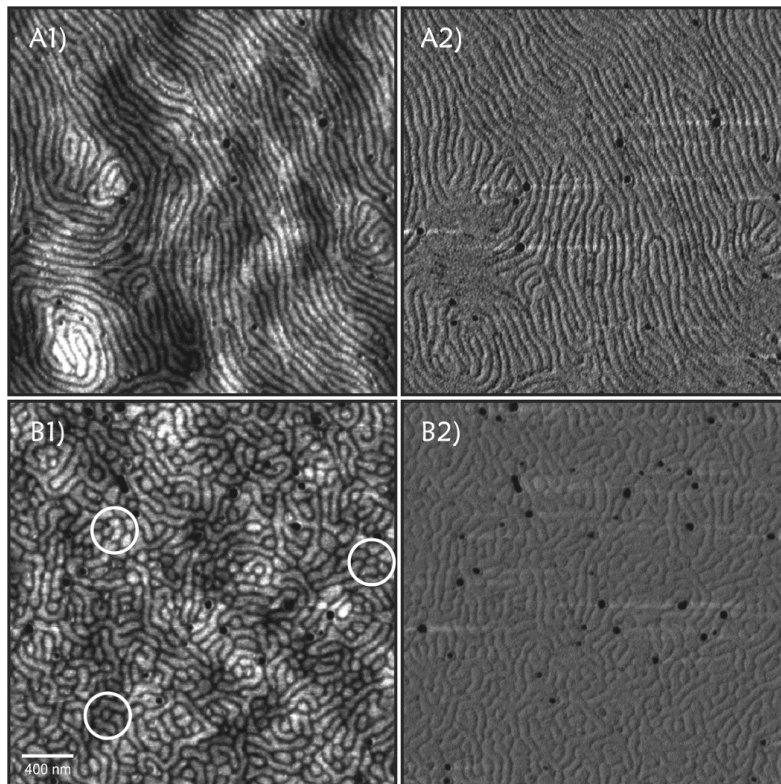


**Figure 4:** AFM (*left*/*right* height/phase) images corresponding to thin films of: a) nanocomposite with 2 wt% and b) 5 wt% of PMMA-grafted nanoparticles after annealing with acetone vapors for 16 h.
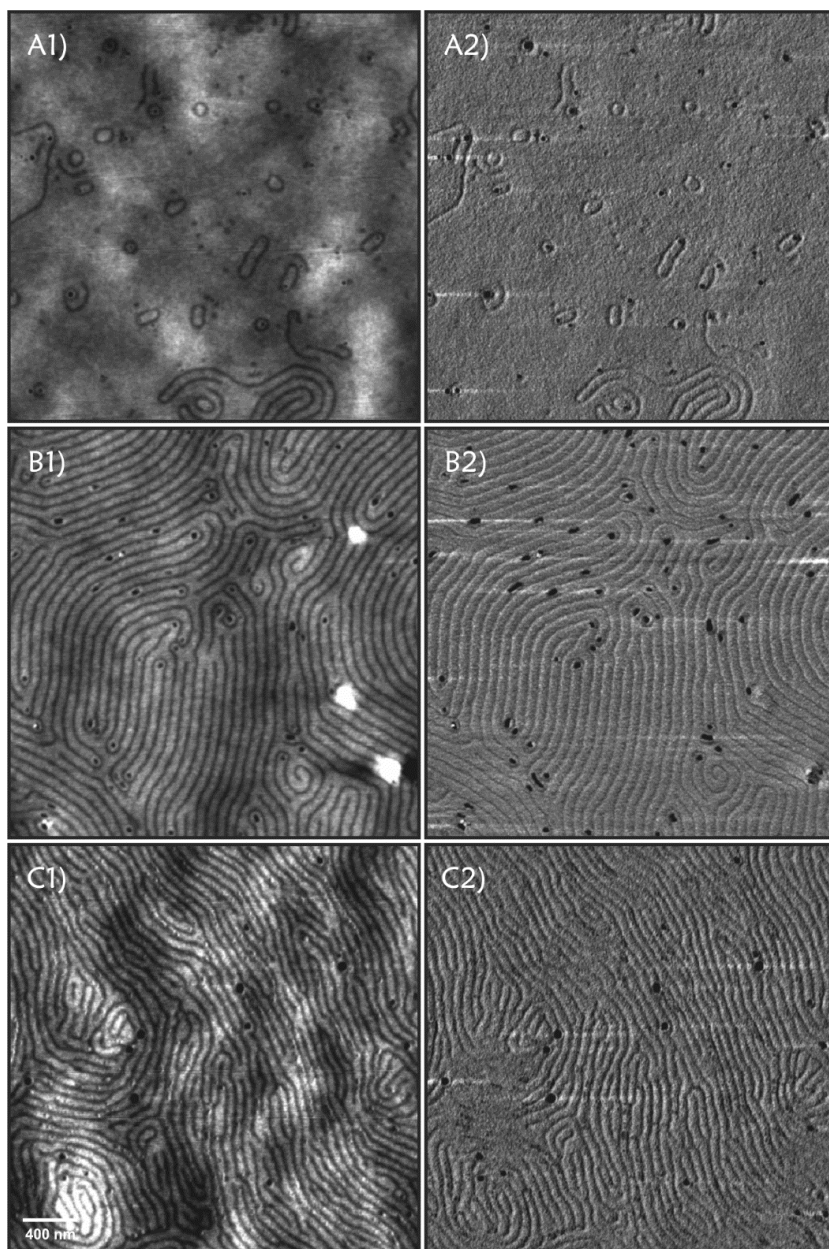
**Figure 5:** AFM (*left*/*right* height/phase) images corresponding to thin films of: a) nanocomposite with 2 wt% of neat nanoparticles, b) nanocomposite with 2 wt% of silanized nanoparticles, and c) nanocomposite with 2 wt% of PMMA-grafted nanoparticles, after annealing with acetone vapors for 16 h.
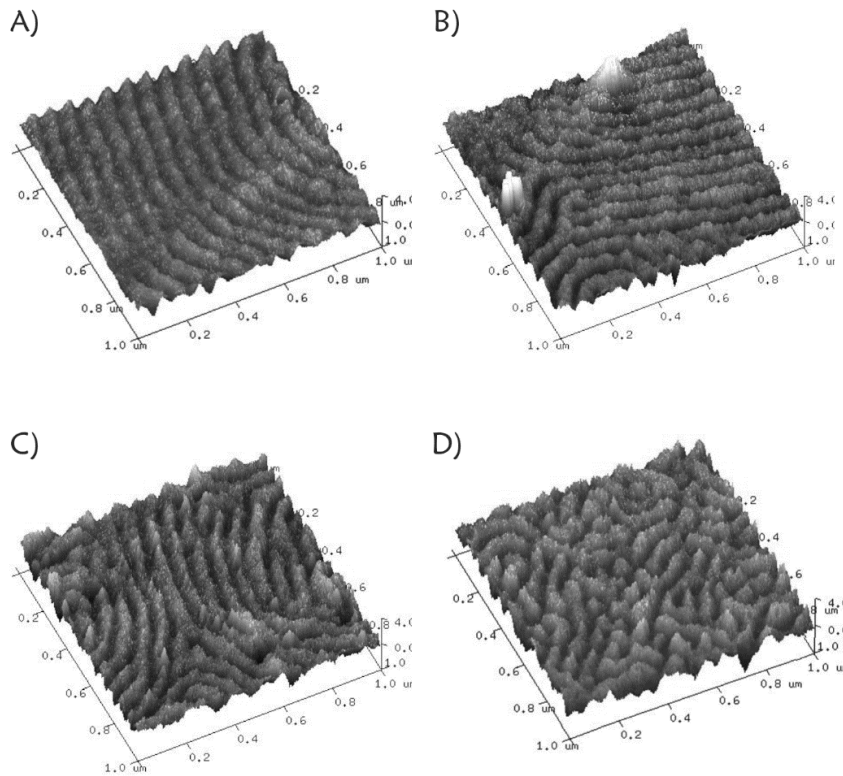
**Figure 6:** AFM 3D height images corresponding to thin films of: a) neat PS-*b*-PMMA copolymer, b) nanocomposite with 2 wt% of silanized nanoparticles, c) nanocomposite with 2 wt% of PMMA-grafted nanoparticles, and d) nanocomposite with 5 wt% of PMMA-grafted nanoparticles, after annealing with acetone vapors for 16 h.
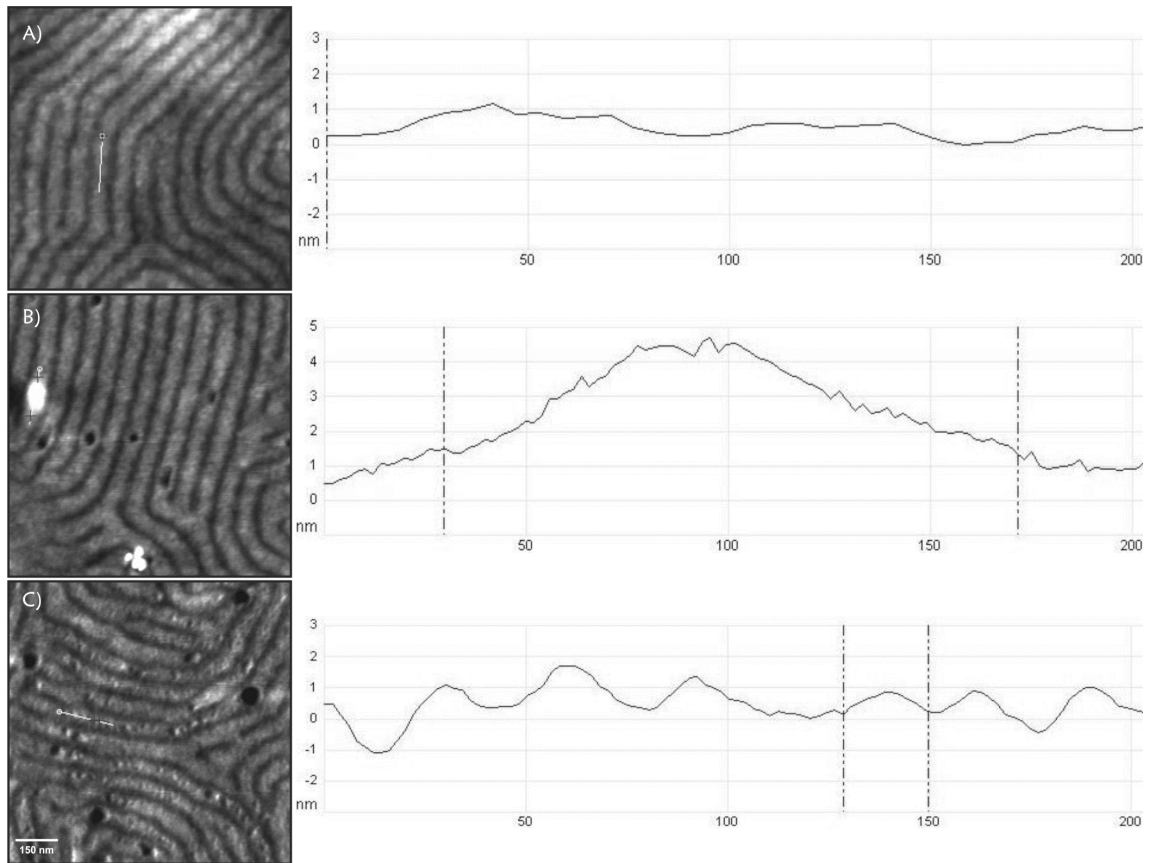
**Figure 7:** AFM height and the profile images of: a) neat PS-*b*-PMMA copolymer, b) nanocomposite with 2 wt% of silanized nanoparticles, c) nanocomposite with 2 wt% of PMMA-grafted nanoparticles.
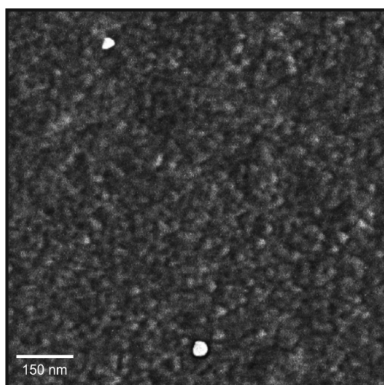


**Figure 8:** AFM phase image corresponding to thin film of the nanocomposite with 5 wt% of PMMA-grafted nanoparticles after thermal degradation of the polymeric matrix.